Hindawi Publishing Corporation
The Scientific World Journal
Volume 2015, Article ID 815084, 8 pages
http://dx.doi.org/10.1155/2015/815084

*Research Article*

# Self-Consolidation Mechanism of Nanostructured $Ti_5Si_3$ Compact Induced by Electrical Discharge

**W. H. Lee,[1] Y. W. Cheon,[1] Y. H. Jo,[1] J. G. Seong,[1] Y. J. Jo,[1] Y. H. Kim,[2] M. S. Noh,[3] H. G. Jeong,[3] C. J. Van Tyne,[4] and S. Y. Chang[5]**

[1]*Faculty of Nanotechnology and Advanced Materials Engineering, Sejong University, Seoul 143-747, Republic of Korea*
[2]*Department of Dental Laboratory Technology, Wonkwang Health Science University, Iksan 570-750, Republic of Korea*
[3]*Center for SCINOVATOR, Posung High School, Seoul 138-829, Republic of Korea*
[4]*Department of Metallurgical and Materials Engineering, Colorado School of Mines, Golden, CO 80401, USA*
[5]*Department of Materials Engineering, Korea Aerospace University, Goyang-si 412-791, Republic of Korea*

Correspondence should be addressed to S. Y. Chang; sychang@kau.ac.kr

Received 30 August 2014; Revised 26 October 2014; Accepted 27 October 2014

Academic Editor: Xiao-Feng Zhao



Electrical discharge using a capacitance of 450 $\mu$F at 7.0 and 8.0 kJ input energies was applied to mechanical alloyed $Ti_5Si_3$ powder without applying any external pressure. A solid bulk of nanostructured $Ti_5Si_3$ with no compositional deviation was obtained in times as short as 159 $\mu$sec by the discharge. During an electrical discharge, the heat generated is the required parameter possibly to melt the $Ti_5Si_3$ particles and the pinch force can pressurize the melted powder without allowing the formation of pores. Followed rapid cooling preserved the nanostructure of consolidated $Ti_5Si_3$ compact. Three stepped processes during an electrical discharge for the formation of nanostructured $Ti_5Si_3$ compact are proposed: (a) a physical breakdown of the surface oxide of $Ti_5Si_3$ powder particles, (b) melting and condensation of $Ti_5Si_3$ powder by the heat and pinch pressure, respectively, and (c) rapid cooling for the preservation of nanostructure. Complete conversion yielding a single phase $Ti_5Si_3$ is primarily dominated by the solid-liquid mechanism.

## 1. Introduction

Syntheses of intermetallic compounds with high melting points via mechanical alloying have been attempted in numerous studies [1, 2]. In general, combustion reactions have been initiated by ball milling in a variety of highly exothermic reaction mixtures. The formation of intermetallics from their elemental components accelerates during ball milling to become a self-sustaining high temperature reaction [3, 4]. Among intermetallic compounds, $Ti_5Si_3$ has attracted more interest recently because a number of their properties have potential in materials applications. Characteristics which make them promising high temperature structural materials include low temperature toughness, high temperature strength and creep resistance, oxidation resistance, and relatively low density [5, 6]. There are various ways to improve the fracture toughness of $Ti_5Si_3$, such as reduction of grain size and alloying with other elements [7–9].

Conventionally, a solid bulk typed $Ti_5Si_3$ can be synthesized by reacting mixed stochiometric powders of Ti and Si at higher temperature or arc melting of Ti and Si pieces [10, 11]. In spite of their research significance, in recent years there have been relatively few studies on the consolidation of $Ti_5Si_3$ in the form of powder. The usual sequence in powder metallurgy operations is to compact a metal powder in a die at room temperature and subsequently sinter it at elevated temperatures. Not only are high pressure, high temperature, and long times required, but in the case of reactive materials, such as Ti and its alloys, an inert atmosphere is also inevitably required. The high temperatures involved in these processes, however, result in detrimental changes in the microstructure and mechanical properties.

Lee and coworkers reported that Ti, Ti-6Al-4V, and $Ti_5Si_3$ powders can be successfully consolidated into a solid bulk type without detrimental changes in the microstructure and mechanical properties by using an electrical discharge

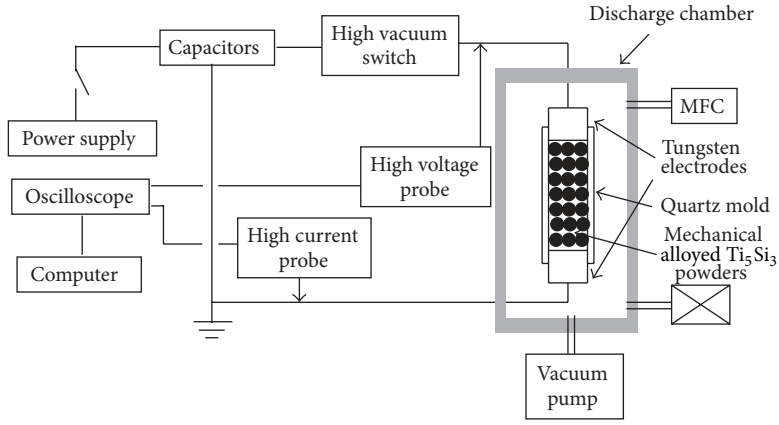


Figure 1: A schematic diagram of the experimental setup for the electrical discharge consolidation (EDC) technique.

technique [12–15]. However, the formation of nanostructured $Ti_5Si_3$ compact by the discharge has not been reported.

This paper thus analyzes the electrical discharge characteristics in terms of input energy, capacitance, and discharge time. It also systematically describes means by which the electrical discharge consolidates the mechanical alloyed $Ti_5Si_3$ powder particles to produce a solid compact with a nanostructure.

## 2. Materials and Methods

Elemental Ti and Si powders were mechanically alloyed (MAed) for 30 minutes at a fixed rpm of 1200 in an Ar atmosphere using a high speed Spex 8000D mixer/mill (SPEX Industries, Inc.) and a cylindrical partially stabilized zirconia (PSZ) vial (60 mm i.d. and 87 mm long) with high Cr hardened steel balls (10.0 and 4.7 mm in diameter). The charged atomic ratio of the reactants corresponded to the reaction stoichiometry (Ti-37.5 at.% Si). The purity of the powders was better than 99.95%. The mass of the powder charge was 10 g and the mass ratio of ball to powder was 5 : 1.

MAed powder without any surface treatment was mounted on the spectrometer probe tip by means of double-sided adhesive tape and examined by XPS (X-ray photoelectron microscopy) for any possible surface modification. Under the current conditions employed, the full width at half maximum (FWHM) of the Ag $3d_{5/2}$ peak was 1.1 eV, and the binding energy difference between Ag $3d_{5/2}$ and Ag $3d_{3/2}$ was 6.0 eV. When the Ag $3d_{5/2}$ peak was used as the reference peak, the binding energy of the C1s peak of adventitious carbon on the standard silver surface was 285 eV. All binding energies were referenced to the C1s peak to correct for sample charging.

0.34 grams of MAed powder was vibrated into a quartz tube with an inner diameter of 4.0 mm that had a tungsten electrode at the bottom and top. The discharging chamber was evacuated to $2 \times 10^{-2}$ torr. A capacitor bank of 450 $\mu$F was charged with two different electrical input energies (7.0 and 8.0 kJ). The charged capacitor bank instantaneously discharged through the MAed powder column without applying any pressure by on/off high vacuum switch which closes the discharge circuit. The voltage and current that the powder column experiences when the circuit is closed were simultaneously picked up by a high voltage probe and a high current probe, respectively. Outputs from these probes are fed into a high speed oscilloscope that stores them as a function of discharge time. The overall process is referred to as electrical discharge consolidation (EDC). A schematic of the EDC apparatus is shown in Figure 1.

The phase compositions of the MAed powder and EDC compacts were investigated by X-ray diffraction (XRD) using Cu $K_\alpha$ radiation. Each EDC compact was sliced every two millimeters and the resulting cross-sections were examined under scanning electron microscopy (SEM) and transmission electron microscopy (TEM). The average hardness values were obtained from at least 20 measurements on the cross-sections of each sample.

## 3. Results and Discussion

Figure 2(a) shows SEM micrograph of the MAed powder with a mean particle size of 3.4 $\mu$m, which was used in current experiment. XRD patterns of the powder, shown in Figure 2(b), confirmed that the powder is mainly composed of $Ti_5Si_3$ phase.

To investigate the surface chemical states of MAed $Ti_5Si_3$ powder, XPS was carried out. Figure 3(a) shows narrow scan spectra of the Ti 2p region before and after light $Ar^+$ etching for 5 minutes. For the MAed $Ti_5Si_3$ powder before etching, a Ti $2p_{3/2}$ peak at 459.2 eV is shown, with 5.8 eV splitting between the Ti $2p_{1/2}$ and Ti $2p_{3/2}$ peaks. The Ti $2p_{3/2}$ peak at 459.2 eV corresponds to $TiO_x$, implying that the surface of MAed $Ti_5Si_3$ powder is primarily in the form of titanium oxide [16, 17]. However, after etching the MAed $Ti_5Si_3$ powder, the Ti $2p_{3/2}$ peak shifted to lower binding energy, 453.4 eV, which indicates the presence of titanium silicide [18]. It can thus be known that the MAed $Ti_5Si_3$ powder was lightly oxidized. Figure 3(b) shows narrow scan spectra of the Si 2p region before and after light $Ar^+$ etching for 5 minutes. For the MAed $Ti_5Si_3$ powder before etching, a Si 2p peak at 102.5 eV corresponds to $SiO_x$ [18]. After etching the MAed $Ti_5Si_3$ powder, the Si 2p peak shifted to

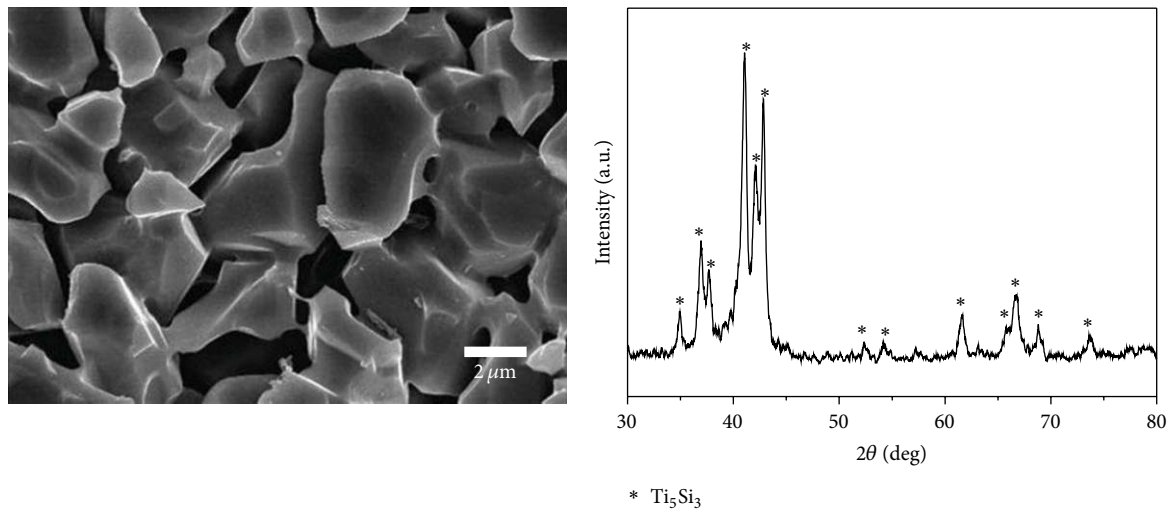


Figure 2: (a) SEM micrograph and (b) XRD patterns of MAed Ti-37.5 at.% Si powder mixture.

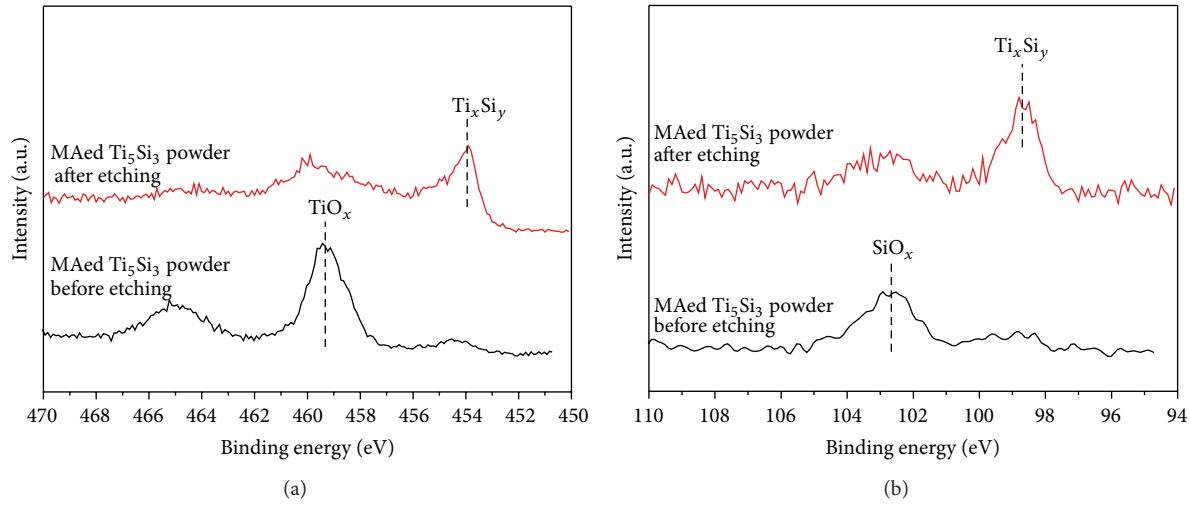


Figure 3: XPS narrow scan spectra of the (a) Ti 2p and (b) Si 2p region of MAed $Ti_5Si_3$ powder before and after light $Ar^+$ etching for 5 minutes.

lower binding energy, 98.2 eV, which indicates the presence of titanium silicide [18]. This result also supports that the MAed $Ti_5Si_3$ powder was lightly oxidized.

The MAed $Ti_5Si_3$ powder was consolidated by a conventional hot-pressing process. As shown in Figure 4(a), the consolidation process at 1200°C in a vacuum of $2 \times 10^{-6}$ torr for two hours by applying a pressure of 10 tons did not successfully produce the compact in a bulk type, resulting in the formation of a porous structure. As listed in Table 1, the hardness of MAed $Ti_5Si_3$ powder was found to be about Hv 1120, but that of the hot-pressed $Ti_5Si_3$ compact decreased down to Hv 800. The decreased hardness can be attributed to the release of strain energy during a hot-pressing and also to the porous structure of the compact. The cross-section views of EDC $Ti_5Si_3$ compacts at the input energy of 7.0 and 8.0 kJ are shown in Figures 4(b) and 4(c), respectively. The compacts were composed of powder particles that were completely deformed and welded together by the electrical discharge. The density of the solid core of EDC $Ti_5Si_3$ compacts is approximately ~99% of theoretical value. From XRD patterns of the EDC $Ti_5Si_3$ compacts as shown in Figure 5, only peaks corresponding to the phase of $Ti_5Si_3$ have been found. It can be known that the unique phase of $Ti_5Si_3$ has not been altered by the electrical discharge process. The average crystallite size of EDC $Ti_5Si_3$ compacts was determined as 93–101 nm by using Suryanarayana and Grant Norton's formula [19]. Measured hardness of EDC $Ti_5Si_3$ compacts is also listed in Table 1, indicating that the hardness can be increased by the electrical discharge.

Figure 6 shows a typical TEM bright-field image (a) and selected area diffraction patterns ((b) and (c)) of the EDC $Ti_5Si_3$ compact discharged at 7.0 kJ of input energy [13].

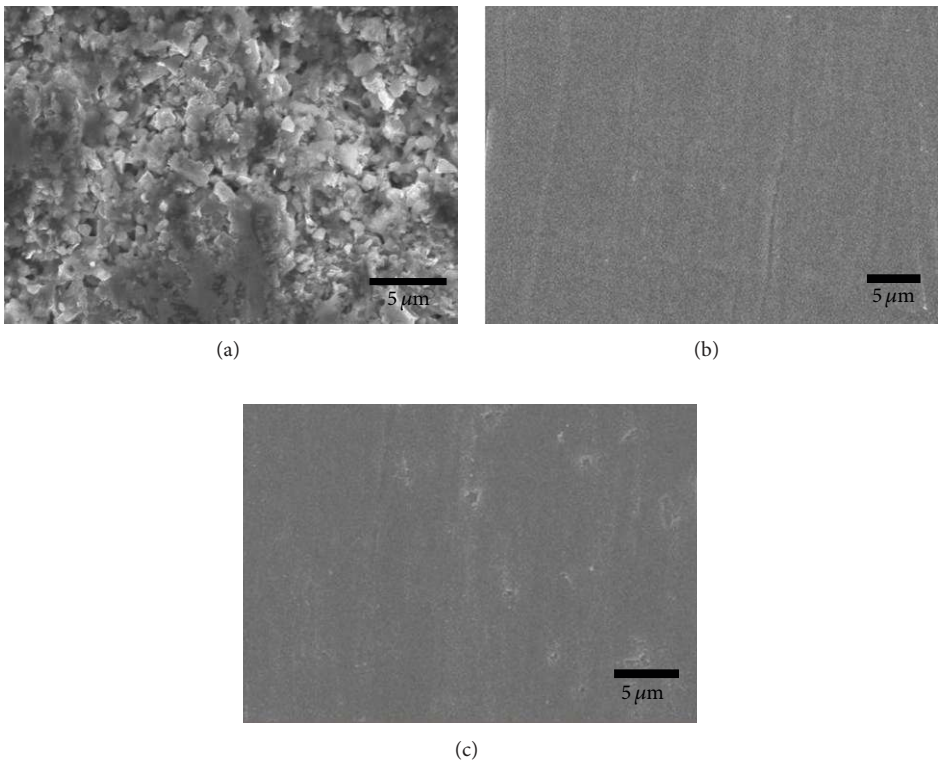


Figure 4: SEM micrographs of the cross-sections of consolidated $Ti_5Si_3$ compacts obtained by (a) hot-pressing at 1200°C in a vacuum of $2 \times 10^{-6}$ torr for two hours with a pressure of 10 tons and electrical discharge consolidation using (b) 7.0 kJ and (c) 8.0 kJ of input energy.

Table 1: Microhardness of MAed $Ti_5Si_3$ powder, hot-pressed $Ti_5Si_3$ compact, and EDC $Ti_5Si_3$ compacts.

| MAed $Ti_5Si_3$ powder | Hot-pressed $Ti_5Si_3$ compact | EDC $Ti_5Si_3$ compact Input energy | |
|---|---|---|---|
| | | 7.0 kJ | 8.0 kJ |
| Hv 1120 | Hv 800 | Hv 1410 | Hv 1450 |

TEM bright-field image in Figure 6(a) presents the facet grain boundary, which is quite flat suggesting that the grain boundaries of the $Ti_5Si_3$ compound are quite stable. The diffraction peaks in Figures 6(b) and 6(c) correspond to [001] and [100] zone axis of hexagonal $Ti_5Si_3$ compound ($P6_3/mcm$), respectively. Based on the analysis of the diffraction patterns, a value of the lattice parameter for the EDC $Ti_5Si_3$ compact can be calculated as $a = 7.42$ Å and $c = 5.17$ Å, which is almost identical to the value of the lattice parameter in the standard hexagonal $Ti_5Si_3$ compound; that is, $a = 7.46$ Å and $c = 5.15$ Å [14]. This indicates that there is no compositional deviation even after the electrical discharge process. This result supports that physical breakdown of the oxide film of MAed powder occurs first in the initial stage of an electrical discharge.

To investigate the consolidation mechanism of nanostructured $Ti_5Si_3$ solid compact by electrical discharge, electrical discharging characteristics were considered in terms

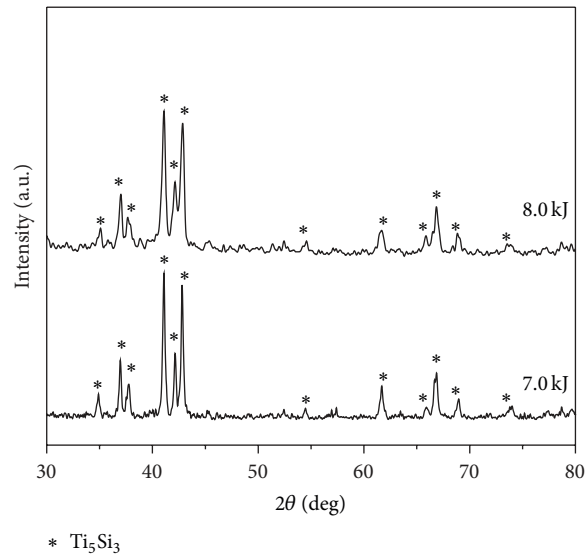


Figure 5: XRD patterns of the $Ti_5Si_3$ compacts obtained by electrical discharge consolidation of MAed $Ti_5Si_3$ powder using 7.0 and 8.0 kJ of input energy.

of input energy and capacitance under current experimental conditions. A typical discharge curve (Figure 7(a)) shows voltage and current in terms of discharge time. 450 μF of capacitance and 5.58 kV of input voltage were employed

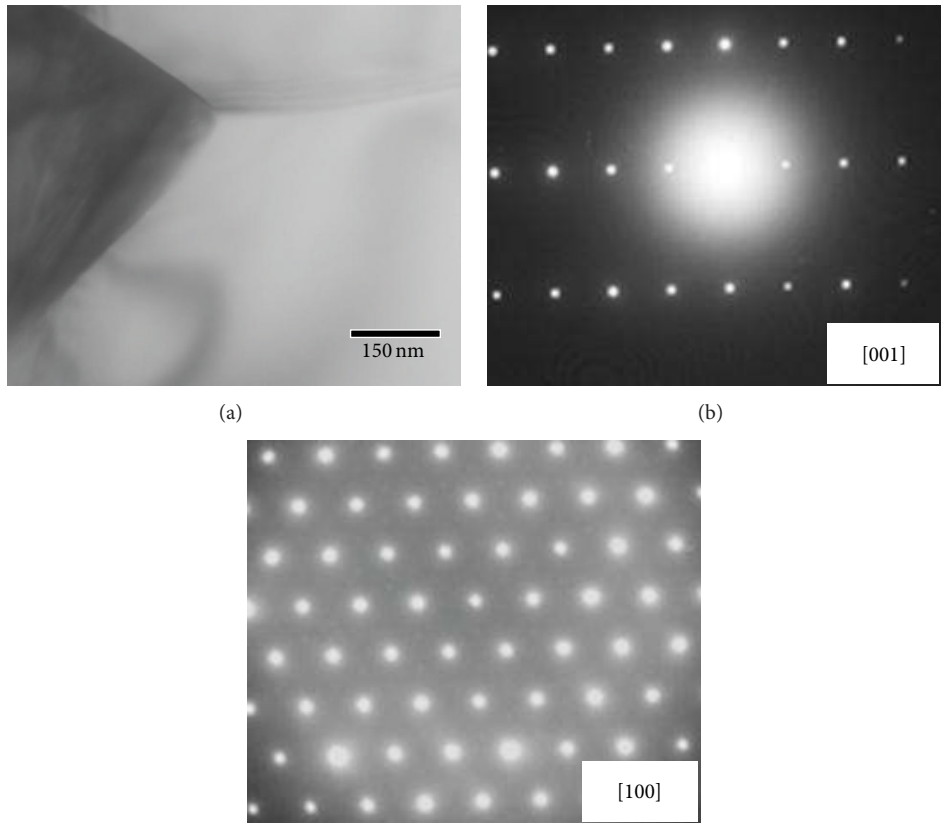


Figure 6: Typical TEM bright-field image (a) and selected area diffraction patterns ((b) and (c)) of the EDC $Ti_5Si_3$ compact at 7.0 kJ of input energy [13].

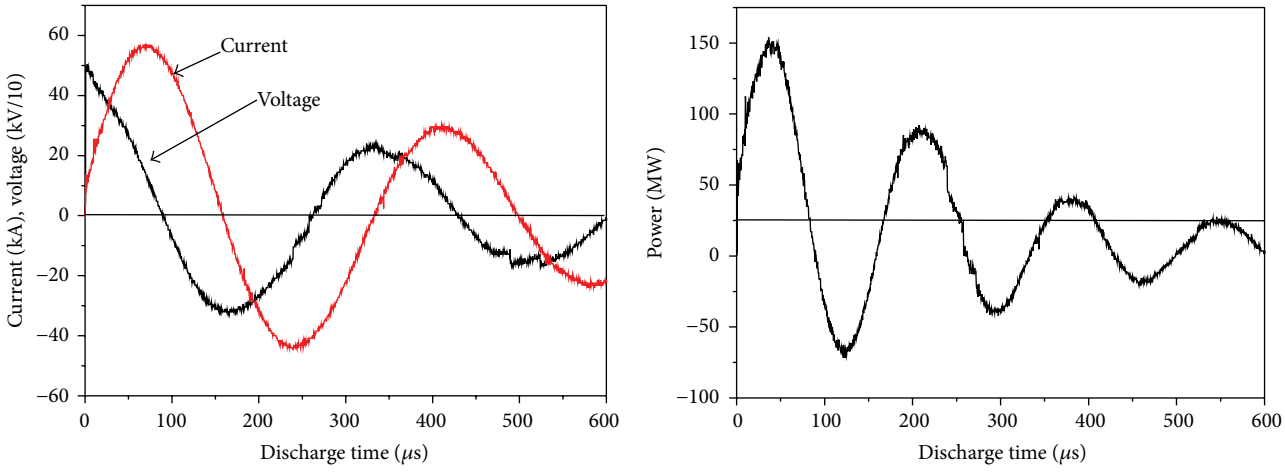


Figure 7: (a) Typical discharge curve measured current and voltage on oscilloscope and (b) typical power curve versus discharge time (discharge condition: 450 $\mu$F, 7.0 kJ).

Table 2: Peak voltage, peak current, discharge time, and heat generated ($\Delta H$) during a discharge.

| Capacitance ($\mu$F) | Input energy (kJ) | Peak voltage (kV) | Peak current (kA) | Discharge time ($\mu$F) | $\Delta H$ (J) |
|---|---|---|---|---|---|
| 450 | 7.0 | 5.04 | 58.4 | 159 | 5880 |
| 450 | 8.0 | 5.36 | 60.8 | 159 | 6640 |

Table 3: Temperature rise ($\Delta T$), current density ($j$), and pinch pressure ($P$) produced by an electrical discharge.

| Input energy (kJ) | Temperature rise (°C) | Current density (A/m$^2$) | Pinch pressure (MPa) |
|---|---|---|---|
| 7.0 | 29,163 | $7.75 \times 10^{11}$ | 300 |
| 8.0 | 33,371 | $8.06 \times 10^{11}$ | 322 |

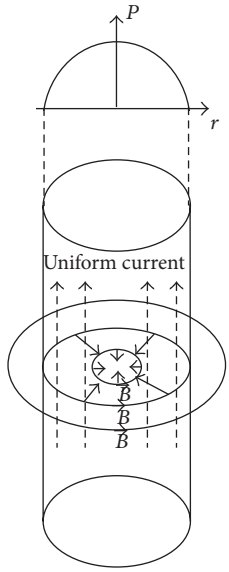


Figure 8: Linear pinch effect with a uniform current distribution.

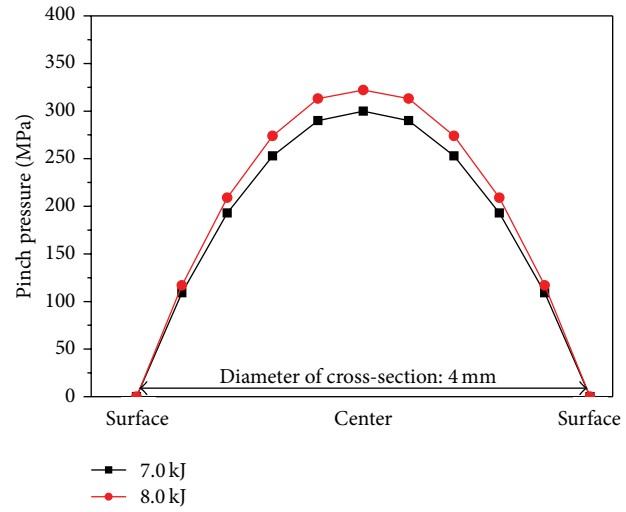


Figure 9: Distribution of pinch pressure generated on the cross-section of EDC $Ti_5Si_3$ compact.

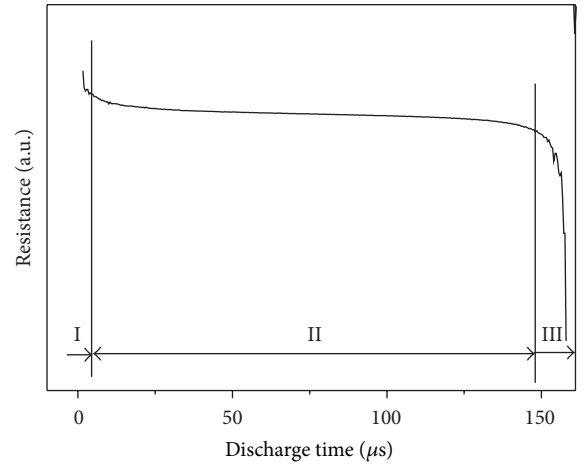


Figure 10: Resistance variation of MAed $Ti_5Si_3$ powder column calculated from the voltage and current recordings during an electrical discharge.

to yield 7.0 kJ. The input energy ($E$) is predetermined by controlling input voltage (V) according to

$$E = \frac{CV^2}{2}, \quad (1)$$

where $C$ is the capacitance of a capacitor. Figure 7(a) shows that the peak current was 58.4 kA and the peak voltage was 5.04 kV. From the results shown in Figure 7(a), the power (watt) curve is plotted in Figure 7(b) against the discharge time. The power was obtained from the following equation:

$$P\,(\text{watt}) = \text{current}\,(\text{A}) \times \text{voltage}\,(\text{V}) = I^2R\ (\text{J/sec}). \quad (2)$$

The discharge times for the duration of the first cycle at two different input energies are identical to be approximately 159 $\mu$sec. The amount of heat generated ($\Delta H$) during a discharge can be obtained by using

$$\Delta H = \sum \left[ i^2(t)\, R(t)\, \Delta t \right]. \quad (3)$$

Typical discharge characteristics under the current conditions are tabulated in Table 2 in terms of peak current, peak voltage, discharge time, and $\Delta H$. It is known that $\Delta H$ increases with an increase in input energy at constant capacitance.

As a usual sintering process, the consolidation of metal powder requires a heat. To understand the effects of $\Delta H$ as one of discharge characteristics for the consolidation process, the temperature rise ($\Delta T$), which is caused by an input energy, is now considered and estimated using

$$W = mCp\Delta T, \quad (4)$$

where $m$ is the mass of the MAed $Ti_5Si_3$ powder and $Cp$ is the specific heat of $Ti_5Si_3$. The electrical input power ($W$) was calculated by integrating current and voltage as a function of discharge time. The resulting data for the heat generated by the electrical discharge process are listed in Table 3. It can be known that the electrical discharge produces the heat

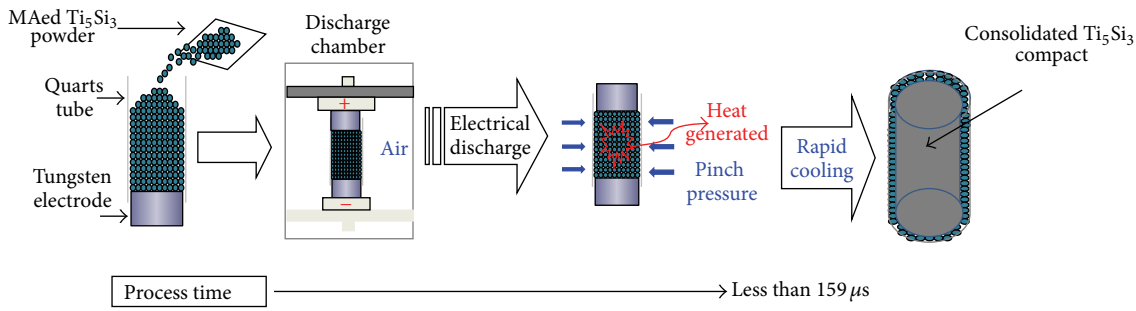


Figure 11: Schematic illustration for the formation of nanostructured $Ti_5Si_3$ compact by an electrical discharge of MAed $Ti_5Si_3$ powder.

significantly greater than the melting temperature of $Ti_5Si_3$. Such a heat generated through the MAed $Ti_5Si_3$ powder is supposed to be high enough to vaporize the $Ti_5Si_3$ powder. However, the duration of the heat rise as 159 $\mu$sec could be too short for the complete vaporization process, resulting in the phase transformation into liquid. Moreover, it can be expected that the consolidated $Ti_5Si_3$ compact contains some pores since the electrical discharge process of $Ti_5Si_3$ powder was carried out without applying any pressure. Therefore, one possible force which can pressurize the liquidus powder can be considered as a function of input energy.

When a capacitor bank is discharged through a powder column, a long cylindrical metal powder column conducting an axial current, distributed axisymmetrically as shown in Figure 8, tends to contract radially inwards. At this moment the magnetic field generated by the current flow causes a diametric contraction, which is known as the pinch effect [20]. The magnitude of the magnetic field ($B$) can be obtained by using

$$B = \frac{1}{2}\mu r j, \tag{5}$$

where $\mu$ is the permeability, $j$ is the current density, and $r$ is the distance from the center of the powder column. The resulting pinch pressure ($P$) is the mechanical force acting on the powder column that will produce a solid core. The pinch pressure is given by

$$P = \frac{\mu j^2 \left(a^2 - r^2\right)}{4}, \tag{6}$$

where $a$ is the radius of the cylindrical powder column. Allow the diameter ($2a$) of the contact region to be approximately one-tenth of the diameter of an average powder particle, as is often the case in solid mechanics [21]. MAed $Ti_5Si_3$ powder particles are considered to be stacked in such a linear manner that only one contact point is formed, resulting in the parallel straight current passage. The geometrical parameters needed for estimating the pinch pressure can be obtained and are tabulated in Table 4. Using these parameters, the maximum pinch pressure can be estimated in the center of the contact area (at $r = 0$). The resulting pinch pressures calculated under current experimental conditions are also listed in Table 3. It can be known that the pinch pressures between 300 and 322 MPa by the discharge were generated and could pressurize the liquidus powder particles, producing a bulk-typed $Ti_5Si_3$ compact without containing pores.

Table 4: Geometric parameters in the pinch pressure calculation.

| | |
|---|---|
| Number of particles on cross-section of powder column | 614 |
| Contact area of particle ($m^2$) | $1.23 \times 10^{-10}$ |
| Mean cross-sectional area of powder particle ($m^2$) | $7.55 \times 10^{-8}$ |
| Radius of the powder column (m) | $1.2 \times 10^{-4}$ |

Since the pinch pressure is maximal at the center of $Ti_5Si_3$ powder column, its distribution across the cross-section of the compact should be different. The distribution of pinch pressures generated across the $Ti_5Si_3$ powder column with two different input energies is shown in Figure 9. The pinch pressure decreases down to 0 at the surface of the $Ti_5Si_3$ powder column. Since the pinch pressure is maximal at the center of the powder column, the solid core is formed easily, especially in the center of the $Ti_5Si_3$ compact. Therefore, it is very logical that the heat generated is the required parameter to melt the MAed $Ti_5Si_3$ powder particles and the pinch pressure can condense them without allowing a formation of pores across the compact.

Figure 10 shows the resistance change through the MAed $Ti_5Si_3$ powder column during an electrical discharge, which was determined from the recordings of voltage and current. It can be seen that there are three distinct regions: 0 to 6 $\mu$sec as stage 1, 7 to 146 $\mu$sec as stage 2, and 147 to 159 $\mu$sec as stage 3. In stage 1, electronic and physical breakdown of the oxide layer of MAed $Ti_5Si_3$ powder occurred, causing the rapid drop of resistance. In stage 2, the resistance decreased very slowly. The heat generated during a discharge would liquefy the MAed $Ti_5Si_3$ powder. Both condensation and densification of melted $Ti_5Si_3$ powder are promoted by the pinch force, especially in the center of the powder column. In stage 3, another rapid drop of resistance occurred. The rapid cooling occurs in this stage, resulting in the preservation of nanosized crystallite of $Ti_5Si_3$ compact.

Figure 11 shows the formation sequence of nanostructured $Ti_5Si_3$ compact by the electrical discharge of MAed $Ti_5Si_3$ powder, indicating that the heat generated, pinch pressure, and rapid cooling are required parameters for the consolidation process of nanostructured $Ti_5Si_3$.

## 4. Conclusions

Electrical discharges of mechanical alloyed Ti-37.5 at.% Si powder mixture using a capacitance of 450 $\mu$F at input energies of 7.0 and 8.0 kJ were carried out without applying any external pressure. The MAed $Ti_5Si_3$ powder was successfully consolidated in times as short as 160 $\mu$sec into a solid bulk of $Ti_5Si_3$ compact with nanosized crystallites. It is proposed that, during an electrical discharge, physical breakdown of the oxide film of MAed $Ti_5Si_3$ powder occurs first. Both melting and condensing the $Ti_5Si_3$ powder are promoted by the heat and the pinch force especially in the center of the powder column, respectively. And then rapid cooling occurred, resulting in the formation of nanostructured $Ti_5Si_3$ compact.

## Conflict of Interests

The authors declare that there is no conflict of interests regarding the publication of this paper.

## Acknowledgment

This research was supported by the Basic Science Research Program through the National Research Foundation of Korea (NRF) funded by the Ministry of Education, Science and Technology (2013R1A1A2010207).

## References

[1] K. Kasraee, A. Tayebifard, and E. Salahi, "Investigation of premilling effect on synthesis of $Ti_5Si_3$ prepared by MASHS, SHS, MA," *Journal of Materials Engineering and Performance*, vol. 22, no. 12, pp. 3742–3748, 2013.

[2] S. Sabooni, F. Karimzadeh, and M. H. Abbasi, "Thermodynamic aspects of nanostructured $Ti_5Si_3$ formation during mechanical alloying and its characterization," *Bulletin of Materials Science*, vol. 35, no. 3, pp. 439–447, 2012.

[3] I.-J. Shon, "Synthesis of $Ti_5Si_{3-x}$ Nb composites by the field-activated combustion method," *Metals and Materials International*, vol. 3, no. 3, pp. 199–202, 1997.

[4] A. K. Vasudevan and J. J. Petrovic, "A comparative overview of molybdenum silicide composites," *Materials Science and Engineering: A*, vol. 155, pp. 1–17, 1992.

[5] R. Rosenkranz, G. Frommeyer, and W. Smarsly, "Microstructures and properties of high melting point intermetallic $Ti_5Si_3$ and $TiSi_2$ compounds," *Materials Science and Engineering A*, vol. 152, no. 1-2, pp. 288–294, 1992.

[6] M. Naka, T. Matsui, M. Maeda, and H. Mori, "Formation and thermal stability of amorphous Ti-Si alloys," *Materials Transactions*, vol. 36, no. 7, pp. 797–801, 1995.

[7] H.-Y. Wang, M. Zha, S.-J. Lü, C. Wang, and Q.-C. Jiang, "Reaction pathway and phase transitions in Al-Ti-Si system during differential thermal analysis," *Solid State Sciences*, vol. 12, no. 8, pp. 1347–1351, 2010.

[8] R. Mitra, "Microstructure and mechanical behavior of reaction hot-pressed titanium suicide and titanium silicide-based alloys and composites," *Metallurgical and Materials Transactions A: Physical Metallurgy and Materials Science*, vol. 29, no. 6, pp. 1629–1641, 1998.

[9] M. Zha, H. Y. Wang, S. T. Li, S. L. Li, Q. L. Guan, and Q. C. Jiang, "Influence of Al addition on the products of self-propagating high-temperature synthesis of Al-Ti-Si system," *Materials Chemistry and Physics*, vol. 114, no. 2-3, pp. 709–715, 2009.

[10] B. R. Krueger, A. H. Mutz, and T. Vreeland, "Shock-induced and self-propagating high-temperature synthesis reactions in two powder mixtures: 5:3 Atomic ratio Ti/Si and 1:1 Atomic ratio Ni/Si," *Metallurgical Transactions A*, vol. 23, no. 1, pp. 55–58, 1992.

[11] S. C. Deevi and N. N. Thadhani, "Reaction synthesis of high-temperature silicides," *Materials Science and Engineering A*, vol. 192-193, no. 2, pp. 604–611, 1995.

[12] W. H. Lee and C. Y. Hyun, "Fabrication of fully porous and porous-surfaced Ti-6Al-4V implants by electro-discharge-sintering of spherical Ti-6Al-4V powders in an one-step process," *Journal of Materials Processing Technology*, vol. 189, no. 1–3, pp. 219–223, 2007.

[13] Y. W. Cheon, Y. J. Jo, C. M. Lee, H. S. Jang, K. B. Kim, and W. H. Lee, "Consolidation of mechanical alloyed Ti-37.5 at.% Si powder mixture using an electro-discharge technique," *Materials Science and Engineering A*, vol. 467, no. 1-2, pp. 89–92, 2007.

[14] H. S. Jang, Y. J. Cho, T. J. Kang, K. B. Kim, and W. H. Lee, "A study on the synthesis and consolidation of $Ti_3Al$ by electro-discharge," *Journal of Korean Institute of Metals and Materials*, vol. 47, no. 8, pp. 488–493, 2009.

[15] Y.-W. Cheon, Y.-J. Cho, T.-J. Kang et al., "Characteristic studies on electro-discharge-sintering of $Ti_5Si_3$ powder synthesized by mechanical alloying," *Journal of Korean Institute of Metals and Materials*, vol. 47, no. 10, pp. 660–666, 2009.

[16] C. Xu and W.-F. Zhu, "Transformation mechanism and mechanical properties of commercially pure titanium," *Transactions of Nonferrous Metals Society of China*, vol. 20, no. 11, pp. 2162–2167, 2010.

[17] M. Rahman, I. Reid, P. Duggan, D. P. Dowling, G. Hughes, and M. S. J. Hashmi, "Structural and tribological properties of the plasma nitrided Ti-alloy biomaterials: influence of the treatment temperature," *Surface and Coatings Technology*, vol. 201, no. 9–11, pp. 4865–4872, 2007.

[18] O. Park, J.-I. Lee, M.-J. Chun et al., "High-performance Si anodes with a highly conductive and thermally stable titanium silicide coating layer," *RSC Advances*, vol. 3, no. 8, pp. 2538–2542, 2013.

[19] W. Kim, S.-H. Kwak, C.-Y. Suh, J.-W. Lim, S.-W. Cho, and I.-J. Shon, "Mechanochemical synthesis and high-frequency induction heated consolidation of nanostructured $Ti_5Si_3$ and its mechanical properties," *Research on Chemical Intermediates*, vol. 39, no. 6, pp. 2339–2349, 2013.

[20] S. Clyens, S. T. S. Al-Hassani, and W. Johnson, "The compaction of powder metallurgy bars using high voltage electrical discharges," *International Journal of Mechanical Sciences*, vol. 18, no. 1, pp. 37–40, 1976.

[21] T. H. Wu, *Solid Mechanics*, Alleyn and Bacon, Boston, Mass, USA, 1976.